Experimental and Molecular Pathology 110 (2019) 104260

Contents lists available at ScienceDirect

Experimental and Molecular Pathology

journal homepage: www.elsevier.com/locate/yexmp

Short report

Sequential treatment failures in response to BRAF/MEK and immune checkpoint inhibitors mediated by MAP2K2 and B2M mutations in melanoma

Craig S. Richmond[a], Yazhini Vallatharasu[b], Jake A. Deviley[c], Cullen R. Vos[a], Benjamin M. Parsons[c], Paraic A. Kenny[a,d,*]

[a] Kabara Cancer Research Institute, Gundersen Medical Foundation, 1300 Badger Street, La Crosse, WI 54601, USA
[b] Department of Medical Education, Gundersen Health System, La Crosse, WI 54601, USA
[c] Department of Oncology, Gundersen Health System, La Crosse, WI 54601, USA
[d] Department of Medicine, University of Wisconsin School of Medicine and Public Health, Madison, WI 53705, USA

ARTICLE INFO

Keywords:
Drug resistance
Metastatic melanoma
Immunotherapy
Whole exome sequencing

ABSTRACT

Although the treatment of metastatic melanoma has been significantly improved by both anti-BRAF/MEK and checkpoint immunotherapies, resistance to these treatment modalities remains a substantial clinical problem. Multiple clinical studies are addressing the optimal sequencing of these agents in larger patient cohorts, but successful long-term individualized treatment will likely require the elucidation of resistance mechanisms from post-progression samples. Here, we describe a patient with BRAF-V600E-positive metastatic melanoma who was sequentially treated with BRAF/MEK inhibitors (dabrafenib/trametinib) and checkpoint inhibitor immunotherapy (nivolumab, followed by pembrolizumab). After the emergence of resistance, whole exome sequencing was performed, implicating *MAP2K2* and *B2M* mutations in loss of response to anti-BRAF/MEK and anti-PD1 therapies, respectively.

1. Introduction

Approximately 96,000 cases of melanoma are diagnosed annually in the United States and it is the leading cause of death from skin cancer (Siegel et al., 2019). Several newer treatments have improved outcomes in patients with metastatic melanoma. Immunotherapies including the anti-CTLA4 antibody ipilimumab (Hodi et al., 2010), followed by anti-PD1 antibodies nivolumab (Weber et al., 2015) and pembrolizumab (Schachter et al., 2017) have significantly improved survival compared to prior therapies. Similarly, the understanding that a substantial fraction of melanomas are driven by mutationally activated BRAF (Davies et al., 2002) led to the approval of BRAF inhibitors such as vemurafenib (Chapman et al., 2011) and the subsequent demonstration of superior efficacy of simultaneously targeting BRAF and MEK (Robert et al., 2015).

Despite these advances, de novo and acquired resistance to immunotherapies and to the small molecule signaling inhibitors remains a significant clinical problem. In the current study, we have performed tumor exome sequencing in a patient sequentially treated with BRAF/MEK inhibitors and anti-PD1 immune checkpoint inhibitors with the goal of elucidating the mechanism(s) of resistance to these agents.

2. Materials and methods

2.1. Whole exome sequencing and PCR

Genomic DNA was isolated from macrodissected formalin fixed paraffin embedded tissue sections using the QIAamp DNA Formalin-Fixed Paraffin Embedded (FFPE) Tissue kit (Qiagen, Germantown MD). Whole exome sequencing was performed by BGI Genomic Services (Hong Kong) on DNA isolated from the immunotherapy-resistant lymph node lesion. Libraries were prepared using the BGI Exome Capture Kit (v4) and sequenced on the BGISeq-500 platform. 178.8 million non-duplicate sequence reads were aligned to the genome using the Burrows-Wheeler Aligner (BWA). The average sequencing depth was 169× on exonic targets. Single nucleotide variants and insertions/deletions were detected using HaplotypeCaller of GATK (v.3.3.0) and annotated using SnpEff (Cingolani et al., 2012) and wAnnovar (Yang and Wang, 2015). Polymerase Chain Reaction to detect the somatic 28 base pair deletion in *B2M* used the following primers, 5'-GGCCTTGTC

* Corresponding author at: Kabara Cancer Research Institute, Gundersen Medical Foundation, 1300 Badger Street, La Crosse, WI 54601, USA.
E-mail address: pakenny@gundersenhealth.org (P.A. Kenny).

https://doi.org/10.1016/j.yexmp.2019.104260
Received 26 February 2019; Received in revised form 11 April 2019; Accepted 9 May 2019
Available online 11 May 2019
0014-4800/

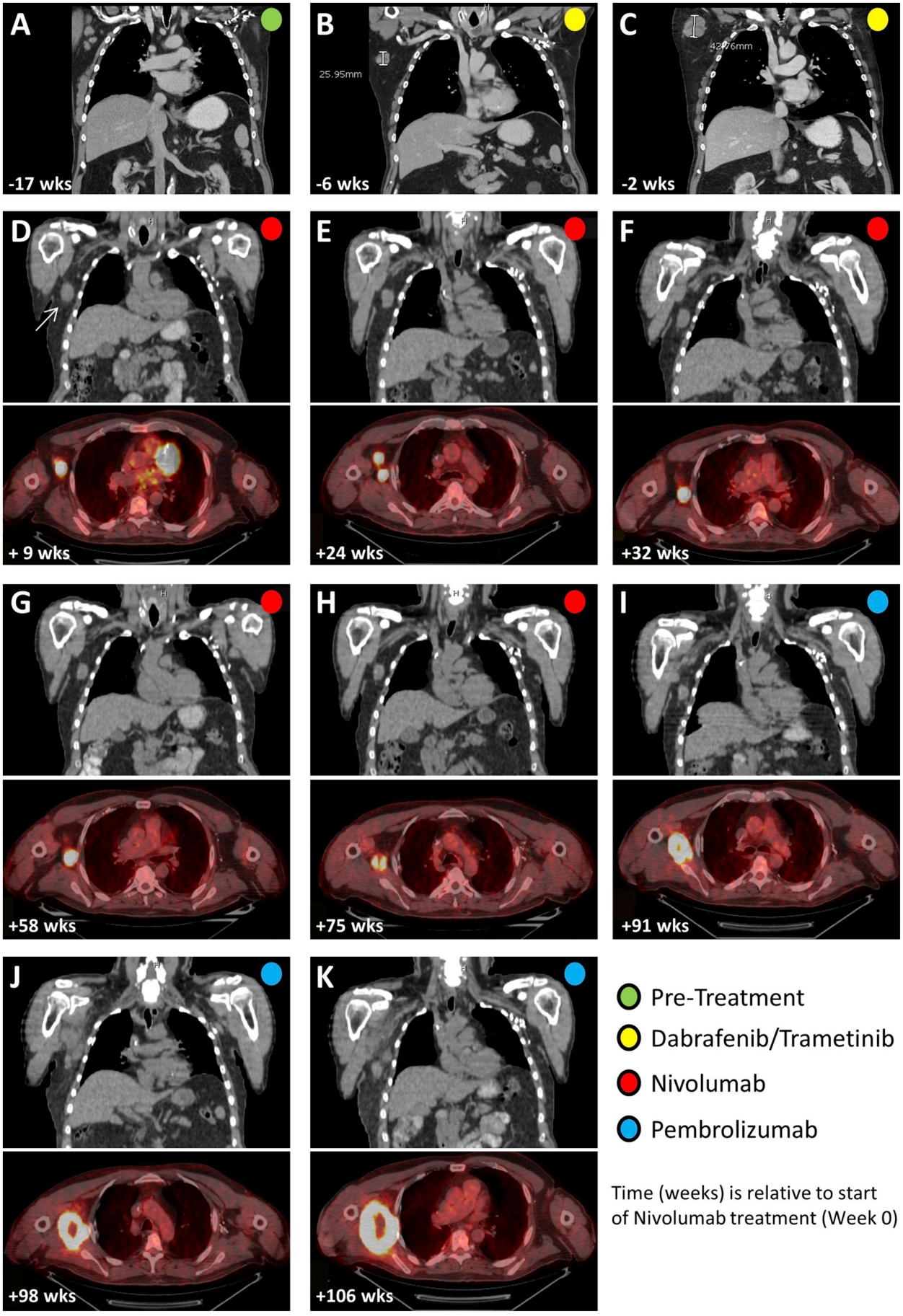

(caption on next page)

Fig. 1. Sequential tumor progression following anti-BRAF/MEK and checkpoint inhibitor treatments. (A–K) Coronal CT images (grayscale) taken at the indicated time points (in weeks, calculated relative to the start of anti-PD1 treatment) highlighting a mass in the right axilla. Axial PET images through the right axillary mass are shown (color, lower panels of D–K) where available.

CTGATTGGCT-3′ and 5'-AGGGTAGGAGAGACTCACGC-3′, which yielded products of 176 bp and 148 base pairs for the wild-type and mutant alleles, respectively. PCR amplicon next generation sequencing (GENEWIZ, South Plainfield, NJ) was also performed to evaluate the presence or absence of key mutations ($BRAF^{V600E}$ and $MAP2K2^{F133L}$) in the original cutaneous lesion using the following primers: BRAF 5'-GATCTACTGTTTTCCTTTACTTACTACACCTC-3′ and 5'-CAGTGGAAAAATAGCCTCAATTCTTACC-3′; MAP2K2 5' GCCTTCATCCCGTTTTCGG-3′ and 5'-CTTCTCCCCAACATGCTCTGTTC-3′.

2.2. Immunohistochemistry

Immunohistochemical detection for B2M was performed on 6-μm sections of formalin-fixed paraffin embedded tumor tissue using the anti-β2-microglobulin (D8P1H) rabbit monoclonal antibody (Cell Signaling Technology, Danvers, MA) at 1:1000 dilution. Antigen retrieval was via 20-min incubation at 95 °C in pH 6.0 citrate buffer and detection was performed with EnVision+ System Horseradish Peroxidase kit (Agilent, Santa Clara, CA) according to the manufacturer's instructions.

2.3. Human subjects

This study was carried out with the approval of the Institutional Review Board of the Gundersen Health System, La Crosse, WI.

3. Results

A male patient in his early sixties presented for evaluation of a progressively enlarging dark and irregularity pigmented papule on the mid-back. Biopsy revealed a non-ulcerated superficial spreading malignant melanoma (Breslow thickness 1.2 mm, Clark level 4, 1.5 × 1.3 × 0.2 cm) without evidence of angiolymphatic or perineural invasion. The patient was treated with wide local excision and sentinel lymph node mapping. One sentinel lymph node was positive for metastatic melanoma. Systemic imaging by PET scan revealed no findings of additional metastatic disease. The patient was stage IIIA (pT2A N1a M0; AJCC 8th Edition). He declined adjuvant treatment.

Four years later, he developed right axillary lymphadenopathy, biopsy of which confirmed $BRAF^{V600E}$-positive recurrent melanoma. A PET/CT scan revealed metastatic disease in the right lower neck, right axilla, left adrenal gland, right upper lobe lung, and multiple bones (Fig. 1A). He was treated with dabrafenib (initially 150 mg twice daily, later reduced to 100 mg twice daily due to fever) and trametinib (2 mg daily). Imaging after 7 weeks of treatment showed a decrease in size and/or stabilization of some lymph node lesions (Fig. 1B), however the patient ultimately progressed in the right axilla after 12 weeks (Fig. 1C).

The patient commenced treatment with the anti-PD1 antibody, nivolumab (3 mg/kg every 2 weeks). Sequential imaging in the weeks prior to initiation of nivolumab showed the progression in the right axilla on dabrafenib/trametinib (Fig. 1C v B), and the response of this index lesion to nivolumab (Fig. 1D–H). After 90 weeks of nivolumab treatment, the patient switched to pembrolizumab, a mechanistically similar PD1 blocking antibody, because of the more convenient dosing schedule (200 mg every 3 weeks, Fig. 1I–K). After a total of 106 weeks on anti-PD1 therapy, the patient progressed (Fig. 1K).

To determine whether genetic mechanisms might underlie the resistance to these targeted therapies, we isolated genomic DNA from a lymph node biopsy obtained post-progression, and from the original cutaneous lesion. The DNA yield from the original lesion was not sufficient for whole exome sequencing so this analysis was restricted to the sample obtained after progression on dabrafenib/trametinib and nivolumab/pembrolizumab. Likely somatic mutations were identified in several cancer relevant genes including *BRAF* (V600E, confirming earlier molecular testing), *NF2* (Y66*), *TP53* (C238F), *MAP2K2* (F133L, see Fig. 2A), *LRP1B* (W1344*).

There are no prior reports of functional characterization of this MAP2K2 mutation, however we note that this region in the kinase domain is highly conserved with MAP2K1 (Fig. 2B) and both of these genes have been reported to be mutated in melanoma (Nikolaev et al., 2011). *MAP2K1* and *MAP2K2* encode the ERK phosphorylating dual specificity kinases MEK1 and MEK2, respectively. The homologous mutation in MAP2K1 (F129L) has been implicated in resistance to MEK inhibitors (Emery et al., 2009; Moriceau et al., 2015). We amplified this region of *MAP2K2* from the original cutaneous lesion and performed massively parallel sequencing on the PCR product to determine whether this mutation was present prior to dabrafenib/trametinib treatment. We achieved 71,966x sequencing depth on this amplicon and did not detect the mutation. In parallel, we confirmed the presence of the $BRAF^{V600E}$ mutation in this sample, thus verifying that there were sufficient neoplastic cells in the DNA preparation to detect the $MAP2K2^{F133L}$ mutation if it was present. In the original study describing *MAP2K1* and *MAP2K2* mutations in treatment-naïve melanoma (Nikolaev et al., 2011), it was noted that the mutational changes (typically somatic C > T or G > A transitions) are typical of ultraviolet light-induced mutations. The $MAP2K2^{F133L}$ variant in this tumor (c.339C > A) is not a typical UV mutation signature, which is perhaps consistent with its emergence later under a drug induced selective pressure. Therefore, we conclude that the $MAP2K2^{F133L}$ mutation most likely developed during the course of therapy. Based on the homology with the functionally characterized MAP2K1 mutation, it seems likely that this variant is a strong candidate to contribute to the acquired resistance to anti-BRAF/MEK therapy in this patient.

In addition, we detected a mutation in the *B2M* gene (Fig. 2C), which encodes beta-2-microglobulin, a protein involved in cell surface antigen presentation. This mutation, a 28 base pair deletion resulting in a frame-shift and truncation starting from codon 3 (NM_004048.2:p.Arg3fs/c.9_36delCTCCGTGGCCTTAGCTGTGCTCGCGCTA), is a loss-of-function mutation. B2M is required for HLA class I folding and transport to the cell surface, and its genetic deficiency has been shown to lead to lack of CD8 T cell recognition. Presence of the deleted *B2M* allele was confirmed by PCR in the post-treatment sample and, notably, was absent from the original lesion (Fig. 2D). Immunohistochemical analysis also showed depletion in the post-immunotherapy specimen (Fig. 2E). The absence of B2M immunostaining in neoplastic cells in the post-treatment specimen (Fig. 2E) and substantial intensity difference between the bands representing deleted and wild-type alleles in the PCR from this specimen implies that the wild-type *B2M* allele has been lost from the tumor cells.

4. Discussion

In this study we used longitudinal analysis of tumor biopsy specimens to determine the mechanisms of resistance to two key modalities in melanoma treatment. A novel mutation in MAP2K2 is described which most likely conferred resistance to dabrafenib and trametinib treatment, while a frameshift mutation in *B2M* was the strongest candidate alteration for progression on checkpoint inhibitor therapy.

Numerous studies have addressed mutations conferring resistance to anti-BRAF therapies, implicating mutations in genes such as *NRAS*, *NF1*, *MITF*, *PIK3CA*, *PTEN*, *PIK3R1*, *RAC1*, *MAP2K1* and *MAP2K2* (Amaral et al., 2017; Van Allen et al., 2014). One *MAP2K2* variant,

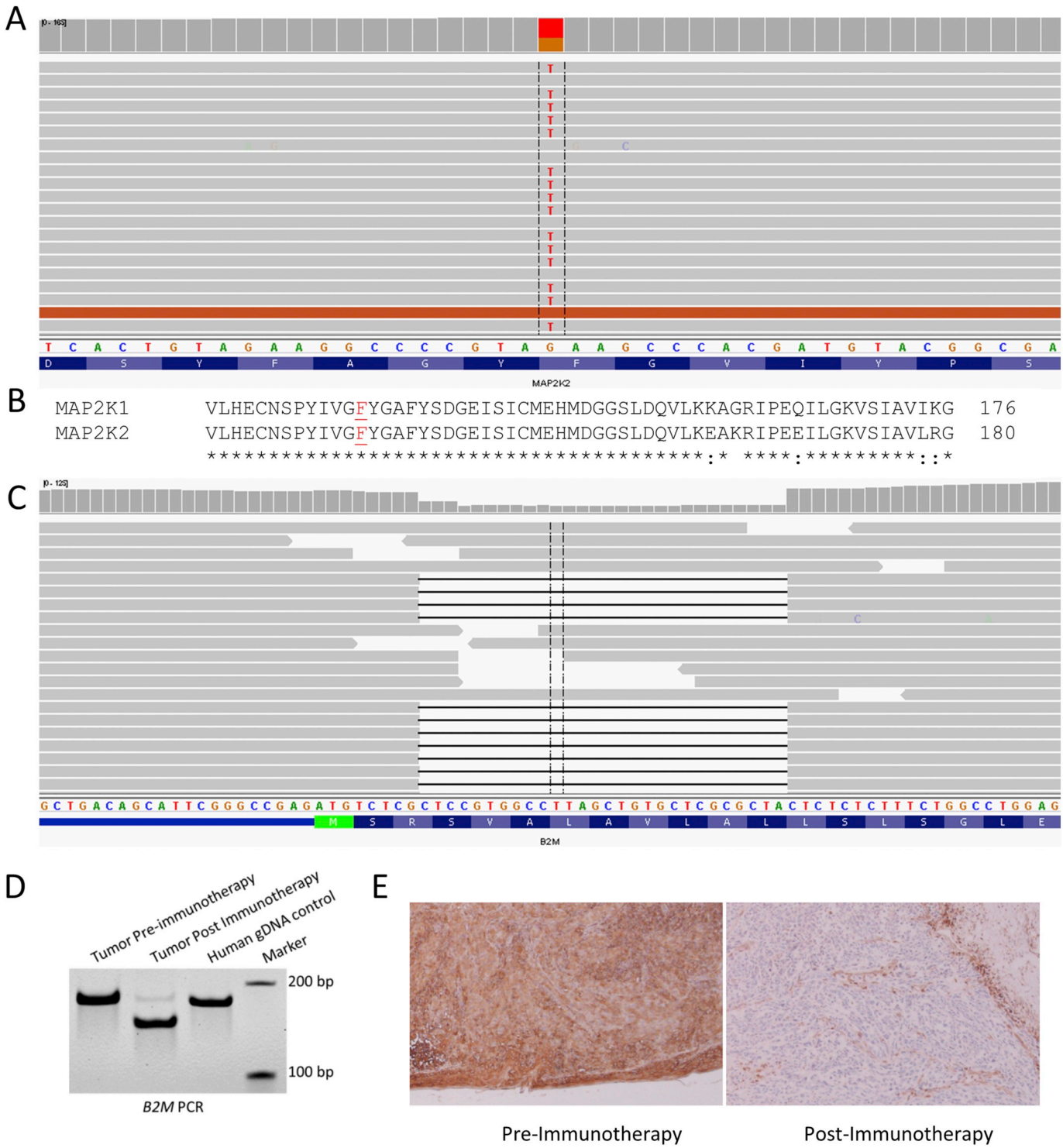

Fig. 2. Identification of candidate mutations mediating escape from anti-BRAF/MEK and checkpoint inhibitor therapy.
A. IGV screenshot from exome sequencing data from the post-progression lymph node specimen showing the mutation in *MAP2K2* which encodes the MAP2K2^{F133L} protein. As MAP2K2 is encoded on the reverse strand, the amino acid sequence shown is read from right to left and the G > T transition shown is equivalent to a c.399C > A transition on the coding (reverse) strand.
B. Partial multiple sequence alignment from the kinase domains of MAP2K1 and MAP2K2 demonstrating the high homology in the region surrounding MAP2K1^{F129}/MAP2K2^{F133} (red).
C. IGV screenshot from exome sequencing data from the post-progression lymph node specimen showing a 28 base pair deletion starting at codon 3 of the *B2M* gene.
D. PCR using primers spanning the 28 base pair deletion region of *B2M* from the pre- and post-immunotherapy treatment specimens demonstrating the absence of the deleted allele pre-treatment and the very pronounced shift to the deleted allele in the post-treatment specimen. An unrelated human genomic DNA sample was used as an additional control to confirm the size of the *B2M*^{WT} product.
E. Immunohistochemistry for B2M protein expression (brown) in pre- and post-immunotherapy specimens demonstrating the loss of B2M in neoplastic cells post-immunotherapy. (For interpretation of the references to color in this figure legend, the reader is referred to the web version of this article.)

MAP2K2^{Q60P}, has been previously implicated in acquired resistance to dabrafenib and trametinib in a melanoma patient (Wagle et al., 2014), while four variants (V35M, L46F, C125S and N126D) were implicated in clinical resistance to vemurafinib (Van Allen et al., 2014). These findings support the hypothesis that the MAP2K2^{F133L} variant detected in our patient might mediate a similar phenotype.

The MAP2K1 variant homologous to MAP2K2^{F133L} (MAP2K1^{F129L}) was detected in a saturation mutagenesis screen of *MAP2K1* for alleles conferring resistance to AZD6244/selumetinib (Emery et al., 2009), which, like other MEK inhibitors in clinical use (trametinib, binimetinib, cobimetinib) is an allosteric inhibitor. Ectopic MAP2K1^{F129L} expression promoted strong ERK1/2 activity in the presence of a MEK inhibitor and reduced sensitivity of cultured cells to both MEK and BRAF inhibition. Specifically, the GI_{50} of A375 cells for selumetinib was increased by 183-fold and the GI_{50} for the vemurafenib-related BRAF inhibitor, PLX4720, was doubled (Emery et al., 2009). One quite comprehensive study evaluating many MAP2K1 mutants (but not including the MAP2K1^{F129L} mutation) highlighted three distinct phenotypic classes of these mutants (Gao et al., 2018), which emphasizes that a very granular understanding of the biologically consequences of specific MAP2K1 (and presumably MAP2K2) mutations will be necessary to guide therapeutic decision making. Evaluation of the activity of mechanistically distinct MEK inhibitors e.g. R05126766 or E6201 (Wu and Park, 2015) against various common MAP2K1/MAP2K2 mutations may provide new treatment approaches to consider in this setting.

The increase in FDG avidity of the axillary tumor coincided with a switch from nivolumab to pembrolizumab (Fig. 2H v I), both of which are antibody-based immune checkpoint inhibitors targeting PD-1. The treatment change occurred 90 weeks after nivolumab initiation. Whether this treatment change contributed to tumor progression or was simply contemporaneous with the progression is not clear. Notably, this 90 week period substantially exceeds the median progression-free survival time for single agent nivolumab observed in melanoma patients in the Checkmate 037 (Hodi et al., 2018) and Checkmate 067 (Larkin et al., 2018) trials. Structural studies have shown the nivolumab and pembrolizumab interact with different sites on PD-1 (Lee et al., 2016), however there is very substantial overlap in their mechanisms of action and pharmacological properties (reviewed in Fessas et al., 2017). Notably, among subsequent lines of therapy, the patient did have a significant response to an ipilimumab/nivolumab combination regimen (not shown). Given the prior progression on anti-PD1 therapy, it is perhaps likely that ipilimumab (anti-CTLA4) was the more active agent in this combination in this case. An ongoing study (SWOG S1616; NCT03033576) is currently investigating whether adding ipilimumab to nivolumab after progression on anti-PD-1 therapy would improve response rates compared to switching to ipilimumab alone.

Multiple mechanisms of escape from immunotherapy have been postulated and/or demonstrated, not all of which require mutation (Kim and Chen, 2016). Based on our exome sequencing data, we cannot formally exclude the possibility that one or more non-mutagenic mechanism might also be contributing. Deletion of *B2M* in mouse models shows that B2M is required for the cell surface expression of MHC class I (Koller et al., 1990). *B2M* mutation has been implicated in acquired resistance to checkpoint inhibitors in recent studies of melanoma (Zaretsky et al., 2016), lung (Gettinger et al., 2017) and colorectal cancer (Le et al., 2017), and also plays a role in mediating resistance to immune surveillance (Bodmer et al., 1993) as well as to earlier generations of immunotherapy (Restifo et al., 1996). Accordingly, this seems to be a common emerging mechanism of resistance and it is likely that it played a significant role in the emergence of anti-PD-1 resistant disease in this patient. We also note that there are several examples of *B2M* loss-of-function mutations across various TCGA studies in treatment-naïve patients, suggestive of a small group of tumors with possible de novo insensitivity to immune checkpoint inhibitors via this mechanism.

An ongoing challenge for both BRAF/MEK and immune checkpoint inhibitors will be the development of early detection methodologies for identification of markers tied to molecular mechanisms responsible for resistance to therapy. A comprehensive enumeration of these recurrent mechanisms of escape may offer the possibility of developing rationally-designed second-line treatment strategies. In addition, next-generation sequencing assessment of circulating DNA (Burgener et al., 2017) or sentinel lesions might offer early indications of treatment failure providing the opportunity to consider a change in treatment. The majority of escape mechanisms for anti-BRAF/MEK therapies are known activating hotspot mutations in proto-oncogenes in this signaling pathway, which suggests that a sequential ctDNA sampling approach may be helpful. Some alterations, however, occur in tumor suppressor genes (e.g. *PTEN* and *NF1*) which are likely to be vulnerable to a wider range of loss-of-function mutations, making NGS approaches somewhat more challenging. Similarly, for checkpoint inhibitor immunotherapies, B2M loss seems to be a recurrent mechanism of resistance but developing NGS assays to comprehensively capture the very large potential number of genetic alterations that could lead to B2M loss-of-function could be challenging. Instead, immunohistochemistry for B2M as we have shown here or FACS analysis for loss of cell surface B2M on circulating tumor cells, may prove to be a useful assessment of clinically relevant tumor evolution in response to checkpoint inhibitor therapy.

Acknowledgements

This work was supported by the Gundersen Medical Foundation and by a gift from the Living for Liz Foundation for the discovery of mechanisms of resistance to immunotherapy. PK holds the Dr. Jon and Betty Kabara Endowed Chair in Precision Oncology. Funding sources had no role in study design, data collection or the decision to submit the article for publication.

References

Amaral, T., et al., 2017. MAPK pathway in melanoma part II-secondary and adaptive resistance mechanisms to BRAF inhibition. Eur. J. Cancer 73, 93–101.
Bodmer, W.F., et al., 1993. Tumor escape from immune response by variation in HLA expression and other mechanisms. Ann. N. Y. Acad. Sci. 690, 42–49.
Burgener, J.M., et al., 2017. Cell-free DNA as a post-treatment surveillance strategy: current status. Semin. Oncol. 44, 330–346.
Chapman, P.B., et al., 2011. Improved survival with vemurafenib in melanoma with BRAF V600E mutation. N. Engl. J. Med. 364, 2507–2516.
Cingolani, P., et al., 2012. A program for annotating and predicting the effects of single nucleotide polymorphisms, SnpEff: SNPs in the genome of *Drosophila melanogaster* strain w1118; iso-2; iso-3. Fly (Austin) 6, 80–92.
Davies, H., et al., 2002. Mutations of the BRAF gene in human cancer. Nature 417, 949–954.
Emery, C.M., et al., 2009. MEK1 mutations confer resistance to MEK and B-RAF inhibition. Proc. Natl. Acad. Sci. U. S. A. 106, 20411–20416.
Fessas, P., et al., 2017. A molecular and preclinical comparison of the PD-1-targeted T-cell checkpoint inhibitors nivolumab and pembrolizumab. Semin. Oncol. 44, 136–140.
Gao, Y., et al., 2018. Allele-specific mechanisms of activation of MEK1 mutants determine their properties. Cancer Discov. 8, 648–661.
Gettinger, S., et al., 2017. Impaired HLA class I antigen processing and presentation as a mechanism of acquired resistance to immune checkpoint inhibitors in lung CANCER. Cancer Discov. 7, 1420–1435.
Hodi, F.S., et al., 2010. Improved survival with ipilimumab in patients with metastatic melanoma. N. Engl. J. Med. 363, 711–723.
Hodi, F.S., et al., 2018. Nivolumab plus ipilimumab or nivolumab alone versus ipilimumab alone in advanced melanoma (CheckMate 067): 4-year outcomes of a multicentre, randomised, phase 3 trial. Lancet Oncol. 19, 1480–1492.
Kim, J.M., Chen, D.S., 2016. Immune escape to PD-L1/PD-1 blockade: seven steps to success (or failure). Ann. Oncol. 27, 1492–1504.
Koller, B.H., et al., 1990. Normal development of mice deficient in beta 2M, MHC class I proteins, and CD8+ T cells. Science 248, 1227–1230.
Larkin, J., et al., 2018. Overall survival in patients with advanced melanoma who received Nivolumab versus Investigator's choice chemotherapy in CheckMate 037: a randomized, controlled, open-label phase III trial. J. Clin. Oncol. 36, 383–390.
Le, D.T., et al., 2017. Mismatch repair deficiency predicts response of solid tumors to PD-1 blockade. Science 357, 409–413.
Lee, J.Y., et al., 2016. Structural basis of checkpoint blockade by monoclonal antibodies in cancer immunotherapy. Nat. Commun. 7, 13354.
Moriceau, G., et al., 2015. Tunable-combinatorial mechanisms of acquired resistance limit the efficacy of BRAF/MEK cotargeting but result in melanoma drug addiction.

Cancer Cell 27, 240–256.
Nikolaev, S.I., et al., 2011. Exome sequencing identifies recurrent somatic MAP2K1 and MAP2K2 mutations in melanoma. Nat. Genet. 44, 133–139.
Restifo, N.P., et al., 1996. Loss of functional beta 2-microglobulin in metastatic melanomas from five patients receiving immunotherapy. J. Natl. Cancer Inst. 88, 100–108.
Robert, C., et al., 2015. Improved overall survival in melanoma with combined dabrafenib and trametinib. N. Engl. J. Med. 372, 30–39.
Schachter, J., et al., 2017. Pembrolizumab versus ipilimumab for advanced melanoma: final overall survival results of a multicentre, randomised, open-label phase 3 study (KEYNOTE-006). Lancet 390, 1853–1862.
Siegel, R.L., et al., 2019. Cancer statistics, 2019. CA Cancer J. Clin. 69, 7–34.
Van Allen, E.M., et al., 2014. The genetic landscape of clinical resistance to RAF inhibition in metastatic melanoma. Cancer Discov. 4, 94–109.
Wagle, N., et al., 2014. MAP kinase pathway alterations in BRAF-mutant melanoma patients with acquired resistance to combined RAF/MEK inhibition. Cancer Discov. 4, 61–68.
Weber, J.S., et al., 2015. Nivolumab versus chemotherapy in patients with advanced melanoma who progressed after anti-CTLA-4 treatment (CheckMate 037): a randomised, controlled, open-label, phase 3 trial. Lancet Oncol. 16, 375–384.
Wu, P.K., Park, J.I., 2015. MEK1/2 inhibitors: molecular activity and resistance mechanisms. Semin. Oncol. 42, 849–862.
Yang, H., Wang, K., 2015. Genomic variant annotation and prioritization with ANNOVAR and wANNOVAR. Nat. Protoc. 10, 1556–1566.
Zaretsky, J.M., et al., 2016. Mutations associated with acquired resistance to PD-1 blockade in melanoma. N. Engl. J. Med. 375, 819–829.